PL-TR-92-2091
Environmental Research Papers, No. 1101

INTEGRAL PROBABILITY OF AURORAL ELECTRON FLUX EVENTS FROM SSJ/4 DMSP F9 ELECTRON MEASUREMENTS

David A. Hardy
Khaled H. Bounar

18 May 1992

Approved for public release; distribution unlimited

Original contains color plates: All DTIC reproductions will be in black and white

PHILLIPS LABORATORY
Directorate of Geophysics
AIR FORCE SYSTEMS COMMAND
HANSCOM AIR FORCE BASE, MA 01731-5000

"This technical report has been reviewed and is approved for publication"

DAVID A. HARDY
Program Manager

E. G. MULLEN
Branch Chief

WILLIAM SWIDER
Deputy Director

This document has been reviewed by the ESD Public Affairs Office (PA) and is releasable to the National Technical Information Service (NTIS).

Qualified requestors may obtain additional copies from the Defense Technical Information Center. All others should apply to the National Technical Information Service.

If your address has changed, or if you wish to be removed from the mailing list, or if the addressee is no longer employed by your organization, please notify PL/TSI, Hanscom AFB, MA 01731. This will assist us in maintaining a current mailing list.

Do not return copies of this report unless contractual obligations or notices on a specific document requires that it be returned.

REPORT DOCUMENTATION PAGE

Form Approved
OMB No. 0704-0188

1. AGENCY USE ONLY (Leave blank)	2. REPORT DATE	3. REPORT TYPE AND DATES COVERED
	18 May 1992	Scientific Interim

4. TITLE AND SUBTITLE
Integral Probability of Auroral Electron Flux Events from SSJ/4 DMSP F9 Electron Measurements

5. FUNDING NUMBERS
PE 62101F
Project 7601
Task 22
Work Unit 01

6. AUTHOR(S)
David A. Hardy
Khaled H. Bounar*

7. PERFORMING ORGANIZATION NAME(S) AND ADDRESS(ES)
Phillips Laboratory (GPSP)
Space Physics Division
Space Particles Environment Branch
Hanscom AFB, MA 01731

8. PERFORMING ORGANIZATION REPORT NUMBER
PL-TR-92-2091
ERP, No. 1101

9. SPONSORING/MONITORING AGENCY NAME(S) AND ADDRESS(ES)

10. SPONSORING/MONITORING AGENCY REPORT NUMBER

11. SUPPLEMENTARY NOTES
* RADEX Inc.
3 Preston Court
Bedford, MA 01730

12a. DISTRIBUTION/AVAILABILITY STATEMENT
Approved for public release
Distribution Unlimited

12b. DISTRIBUTION CODE

13. ABSTRACT (Maximum 200 words)

A study has been completed to determine the probability of observing different levels of auroral electron precipitation both within fixed spatial elements in magnetic local time and corrected geomagnetic latitude, and within spatial elements when the magnetic local time is fixed but the latitude range can be varied. The auroral electron precipitation probability is defined for a series of thresholds in electron average energy and electron energy flux as a function of geomagnetic activity. The study provides the capability to determine the probability of observation of an auroral electron precipitation event for any specified threshold in average energy, energy flux, and level of geomagnetic activity for any location in the auroral region or for any line of sight through the auroral region. The input for the study is one year of data from the SSJ/4 electron and proton spectrometer flown on the F9 satellite of the Defense Meteorological Satellite Program (DMSP) comprising approximately 10,141 hemispheric passes through the auroral region. The binning technique used to determine these probabilities is presented and some results are discussed. The operation of the software package to display the probability results is described.

14. SUBJECT TERMS	15. NUMBER OF PAGES
Defense Meteorological Satellite Program (DMSP), Aurora, Precipitating electrons, Geomagnetic Kp index, Integral probability	34
	16. PRICE CODE

17. SECURITY CLASSIFICATION OF REPORT	18. SECURITY CLASSIFICATION OF THIS PAGE	19. SECURITY CLASSIFICATION OF ABSTRACT	20. LIMITATION OF ABSTRACT
Unclassified	Unclassified	Unclassified	Unlimited

Contents

Illustrations

Tables

Acknowledgements

We are grateful to a number of colleagues who have made several suggestions for improving the presentation of this material. We also thank William McNeil for several helpful comments.

Integral Probability of Auroral Electron Flux Events from SSJ/4 DMSP F9 Electron Measurements

1. INTRODUCTION

Determination of the global pattern of auroral particle precipitation is important both for the understanding of the physical processes producing and maintaining the auroral oval and for the prediction of the effects of auroral particle precipitation on operational Air Force systems. For this reason, an extensive set of studies has been conducted to quantify the global pattern using measurements from the SSJ/3 and SSJ/4 particle spectrometers flown on the spacecraft of the Defense Meteorological Satellite Program (DMSP) [1,2,3,4,5,6,7] These studies

---

Received for Publication 18 May 1992

[1] Hardy, D.A., Gussenhoven, M.S. and Holeman, E. (1985) A statistical model of auroral electron precipitation, *J. Geophys. Res.*, **90**:4229.

[2] McNeil, W.J., Hardy, D.A., and O'Neil, R.R. (1984) Private communication, 4 September.

[3] McNeil, W.J., and Hardy, D.A. (1985) Private communication, 17 October.

[4] Hardy, D.A., Gussenhoven, M.S., Raistrick, R. and McNeil, W.J. (1987) Statistical and functional representations of the pattern of auroral energy flux, number flux, and conductivity, *J. Geophys. Res.*, **92**:12275.

[5] Hardy, D.A., Gussenhoven, M.S. and Brautigam, D. (1989) A statistical model of auroral ion precipitation, *J. Geophys. Res.*, **94**:370.

[6] Hardy, D.A., McNeil, W.J., Gussenhoven, M.S. and Brautigam, D. (1991) A statistical model of auroral ion precipitation 2. functional representation of the average patterns, *J. Geophys. Res.*, **96**:5539.

[7] Brautigam, D.H., Gussenhoven, M.S. and Hardy, D.A. (1991) A statistical study on the effects of IMF B_z and solar wind speed on auroral ion and electron precipitation, *J. Geophys. Res.*, **96**:5525.

have been of two types: 1) studies where the behavior of the average electron and ion spectrum is determined as a function of either the level of geomagnetic activity or the value of solar wind parameters, and 2) studies where the probability of occurrence of different levels of auroral precipitation is determined as a function of the level of geomagnetic activity.

The DMSP data set is well suited for such studies because of its size. The SSJ/3 and SSJ/4 detectors are operated continuously on the DMSP satellites, recording complete electron and ion spectra once per second. Approximately 15 years of the data is available, consisting of approximately 150 million spectra. Such a large data set allows determination of the averages and probability distribution to a high precision.

The present study is an extension of this work. This study uses the 1990 measurements from the F9 satellite taken in the 1030-2230 meridian. The purpose of this study is to determine not only the probability of observing a specified level of auroral precipitation at a given spatial location, but also the integral probability of observing this same level over a range in latitude starting from a particular location. Only the first part of these issues was addressed in earlier studies of DMSP data from satellites F2 and F4.[3] The results of such a study allow the determination of the integral probability of occurrence for auroral precipitation events above any specified level in integral energy flux and average energy for any line of sight through the auroral region. This is an important tool for determining background and interference signals for any system operating in the auroral region.

2. ANALYSIS TECHNIQUE

The purpose of this study is to determine the probability of observing auroral electron precipitation at a specified intensity, spectral hardness, and level of geomagnetic activity both at a specific location in the oval, and integrated over any path through the auroral oval. The data for this study are from the SSJ/4 sensor on the DMSP/F9 spacecraft. All data taken in 1990 were used in the study. The F9 satellite is in a circular sun synchronous orbit in the 1030-2230 magnetic meridian at an altitude of approximately 840 kilometers. The spatial coverage of the F9 orbit in a corrected geomagnetic latitude (CGL) magnetic local time (MLT) coordinate system is shown in Figure 1.

For this study we constructed a series of spatial arrays. In each such array we divided the high latitude region into 8 three-hour sectors in MLT. Each array covered the latitude range from 50° to 90° CGL. One such array was constructed for each of six thresholds in integral energy flux and average energy (spectral hardness) and for four levels of geomagnetic activity as measured by Kp. Thus there were a total of 144 arrays (6 thresholds in integral energy flux times 6 thresholds in average energy times 4 Kp ranges). The thresholds, Kp ranges, and spatial bins used are listed in Table 1. The equivalent radiance bins are set assuming that an

electron energy input of 1 erg/cm^2-sec produces 1 kilo-Rayleigh of luminosity at a wavelength of 3969 Å [Figure 12.19, Chapter 12, in Reference 8].

Table 1. Input Parameter Ranges and Bins

Parameter	Bins
Energy flux thresholds	(1) 0.5 (2) 1.6 (3) 5.0 (4) 16.0 (5) 50.0 6) 160.0 (kR)
	(1) 10^8 (2) $10^{8.5}$ (3) 10^9 (4) $10^{9.5}$ (5) 10^{10} (6) $10^{10.5}$ KeV/(cm^2-sec-str)
Average energy thresholds (KeV)	(1) 1.0 (2) 3.0 (3) 7.0 (4) 10.0 (5) 13.0 (6) 17.0
MLT sector (hours)	(1) 0 - 3 (2) 3 - 6 (3) 6 - 9 (4) 9 - 12 (5) 12 - 15 (6) 15 - 18 (7) 18 - 21 (8) 21 - 24
Kp ranges or midnight Equatorward Boundary (MEB in °)	Kp (1) 0_0 - 1+ (2) 2- - 3+ (3) 4- - 5+ (4) 6- - 9_0
	MEB (1) 67.8 - 65.7 (2) 63.7 - 61.6 (3) 59.5 - 57.5 (4) 55.4 - 51.24
Latitude zones	20 latitude bins from 50° to 90° with 2° increments

In each MLT sector of each array we constructed a 20 x 20 matrix. The diagonal elements of the matrix represent the probability of seeing an electron precipitation event above the thresholds for that array during a pass over the auroral zone. The 20 diagonal elements cover the latitude range from 50 to 90° CGL in 2° steps. For a given row in the matrix, the elements to the left of the diagonal represent the integral probability of seeing an event above the thresholds for that array integrated from the latitude of the diagonal to a latitude equatorward of that latitude. Each individual position to the left represents an additional integration over 2° of latitude equatorward. Similarly, the elements to the right represent the integral probability poleward of the latitude of the diagonal element.

The values in the matrix were determined as follows: For each auroral pass, the integral energy flux and average energy are calculated for each 1-second spectrum returned by the SSJ/4 detector. We assume that the pattern of auroral electron precipitation is time stationary over the period of the auroral pass. Based on the values of the integral energy flux and average energy flux calculated, along with Kp at the time the spectrum was taken, we determined to which if any of the arrays the event was to be assigned. Based upon the MLT, the appropriate matrix was chosen and for that matrix the CGL is used to determine the

---

[8] Jursa, A.S., Scientific Editor (1985) *Handbook of Geophysics and the Space Environment*, Chapter 12, AFGL-TR-85-0315, AD A167000

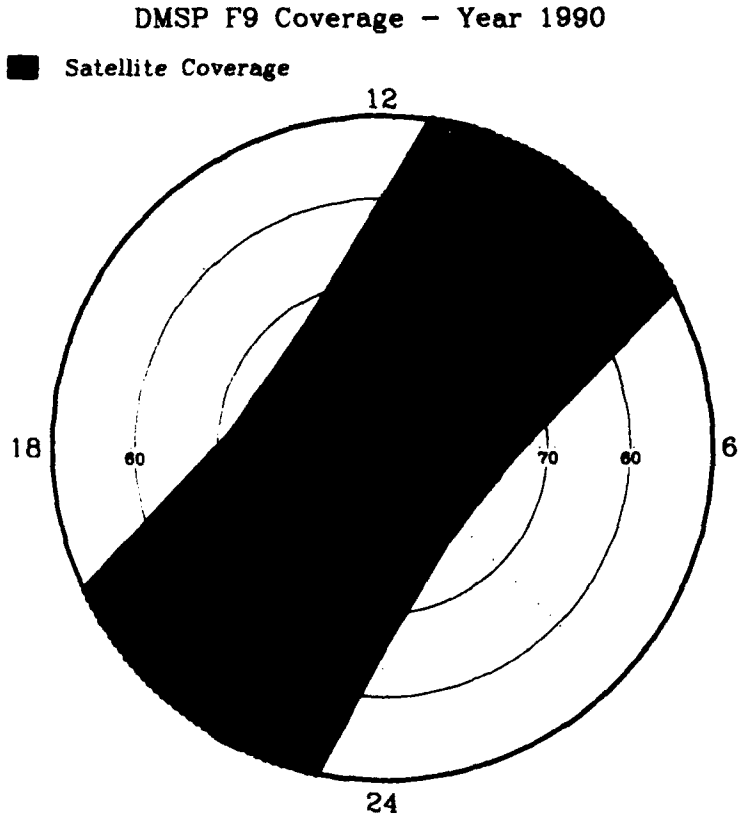

Figure 1. DMSP F9 Satellite Coverage in 1990

correct diagonal element to which the event applies. If the spectrum measured is the first spectrum for that pass observed for that set of thresholds and MLT and for that diagonal element, then we increment the counter for that diagonal element by one. If for that pass a spectrum for that latitude and MLT has already been observed above the thresholds, then the spectrum is ignored and the next spectrum is analyzed. If the diagonal element is incremented by one, we also increment by one all elements of the matrix for the row and column containing the diagonal element. The elements of the row are incremented because if we see an event, for a given pass, that satisfied the threshold requirements in one latitude zone, then starting at that latitude and integrating spatially either equatorward or poleward the probability of seeing an event for that pass must be unity. Similarly, the column is incremented because starting at any other latitude for that pass and integrating either poleward or equatorward, the probability must be unity if the integral extends to the latitude where the event satisfying the thresholds was observed. The spectra taken within one auroral pass will contribute to a number of different arrays and one spectrum can contribute to more than one array. For each pass, a counter for each MLT sector in each array is incremented if, for that pass, that satellite passed through that MLT sector. The desired probabilities are calculated by dividing the values in the matrix by the number of passes occurring in that MLT sector .

A simplified case is used to illustrate the procedure. A simplified latitudinal profile of the integral energy flux is shown in Figure 2. For the purpose of this demonstration we assume that all the electron spectra in the pass have an average energy of greater than 1 keV, that the satellite is in the 2100-2400 MLT sector and that Kp is in the range from 2- to 3+. For this pass we will determine the inputs to the matrix for the integral energy flux greater than 3.16×10^8 keV/(cm^2 sec ster). In the figure, vertical lines are drawn at the 2° intervals corresponding to each of the diagonal elements. A horizontal line is drawn representing the threshold for the matrix. From the figure we determine that for each 2° element in latitude only between 62 and 70° CGL is there at least 1 second in each element when the integral energy flux was above the threshold. The five diagonal elements for this latitude range are incremented by one and the rows and columns are filled in as described in the previous example. This is shown in Table 2.

For such a simplified case we can test whether the matrix produces the correct integral probabilities. If we ask, "what is the probability of seeing an event above threshold at 50° CGL?", it corresponds to the matrix element in the extreme lower-left corner in Table 2. This is zero, in agreement with Figure 2. To determine the integral probability as we move to higher latitude starting at 50° CGL we must consider the lowest row. This integral probability is zero until the sixth column and unity thereafter. This is again consistent with the figure. From 50° CGL poleward, no event above the threshold is seen at latitudes less than 60°. This corresponds to the first five columns which are indeed zero. Since the threshold is exceeded between 60 and 62° CGL, the integral probability from 50° to any latitude above 60° will be unity as is the case in the matrix.

This same procedure was repeated for all auroral passes of the F9 DMSP satellite occurring in 1990. This represented 10,141 auroral passes and a total of over 12 million individual 1-second spectra. This data set was of sufficient size that a good statistical determination was

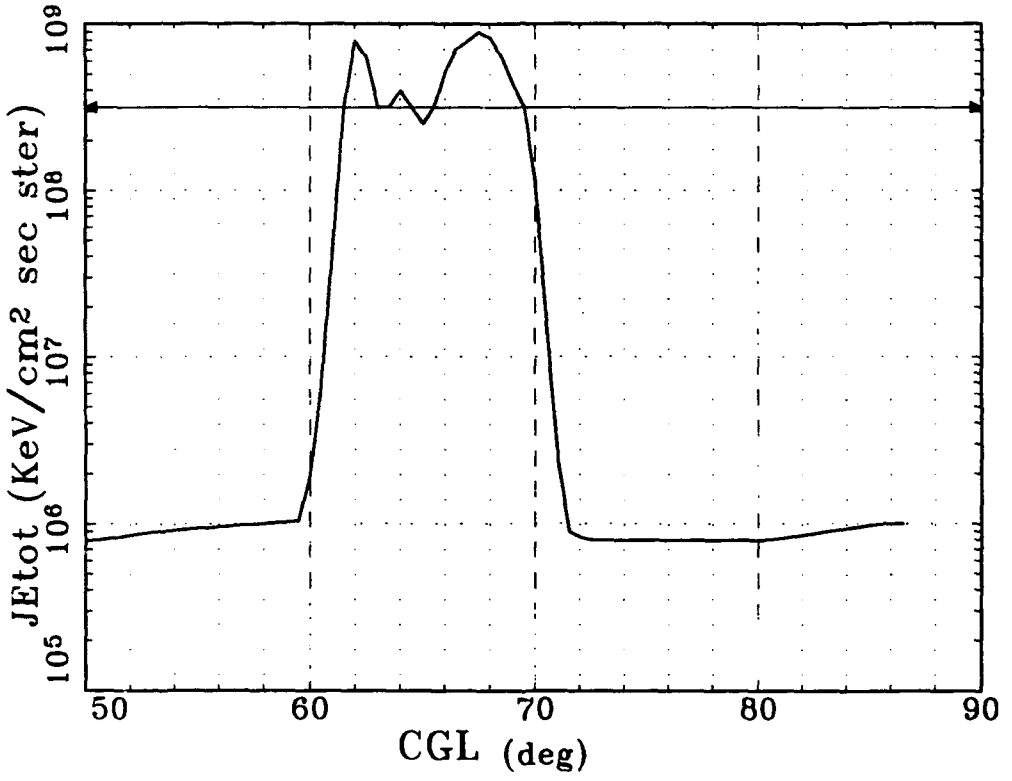

Figure 2. Energy Flux (JE_{tot}) Spectrum for a 1/4 Satellite Orbit (or 1/2 Hemispheric Pass). JE_{tot} is given in KeV/(cm^2 sec ster) as a function of corrected geomagnetic latitude (CGL).

Table 2. Probability Matrix (i,j) for One Pass Through the Auroral Oval

20	1	1	1	1	1	1	1	1	1	1	0	0	0	0	0	0	0	0	0	0
19	1	1	1	1	1	1	1	1	1	1	0	0	0	0	0	0	0	0	0	0
18	1	1	1	1	1	1	1	1	1	1	0	0	0	0	0	0	0	0	0	0
17	1	1	1	1	1	1	1	1	1	1	0	0	0	0	0	0	0	0	0	0
16	1	1	1	1	1	1	1	1	1	1	0	0	0	0	0	0	0	0	0	0
15	1	1	1	1	1	1	1	1	1	1	0	0	0	0	0	0	0	0	0	0
14	1	1	1	1	1	1	1	1	1	1	0	0	0	0	0	0	0	0	0	0
13	1	1	1	1	1	1	1	1	1	1	0	0	0	0	0	0	0	0	0	0
12	1	1	1	1	1	1	1	1	1	1	0	0	0	0	0	0	0	0	0	0
11	1	1	1	1	1	1	1	1	1	1	0	0	0	0	0	0	0	0	0	0
10	1	1	1	1	1	1	1	1	1	1	1	1	1	1	1	1	1	1	1	1
9	1	1	1	1	1	1	1	1	1	1	1	1	1	1	1	1	1	1	1	1
8	1	1	1	1	1	1	1	1	1	1	1	1	1	1	1	1	1	1	1	1
7	1	1	1	1	1	1	1	1	1	1	1	1	1	1	1	1	1	1	1	1
6	1	1	1	1	1	1	1	1	1	1	1	1	1	1	1	1	1	1	1	1
5	0	0	0	0	0	1	1	1	1	1	1	1	1	1	1	1	1	1	1	1
4	0	0	0	0	0	1	1	1	1	1	1	1	1	1	1	1	1	1	1	1
3	0	0	0	0	0	1	1	1	1	1	1	1	1	1	1	1	1	1	1	1
2	0	0	0	0	0	1	1	1	1	1	1	1	1	1	1	1	1	1	1	1
1	0	0	0	0	0	1	1	1	1	1	1	1	1	1	1	1	1	1	1	1
$\frac{j}{i}$	1	2	3	4	5	6	7	8	9	10	11	12	13	14	15	16	17	18	19	20

obtained of both the probability of occurrence above the threshold at individual latitude zones with the MLT coverage of the satellite and also for the probability integrated over latitude.

3. RESULTS

Figure 3 shows a typical example of the output of the study. This figure is generated using the software package EPDF9. A step-by-step guide to the operation of this software is provided in the Appendix. The case shown is for an average energy greater than 7 keV, an integral energy flux greater than 50 erg/(cm^2 sec) (or 50 kR), for the 2100-2400 MLT sector, and for Kp in the range from 2- to 3+. The rectangular section is a color spectrogram of the results. The y axis gives the delta latitude equatorward or poleward of a specific latitude over which the probability is integrated. The x axis gives the latitudes from 50 to 90° CGL within the specified MLT sector. Along the zero delta latitude line, the color scale gives the probability of observing an event above the threshold in each 2° latitude zone. For each CG latitude, the color scaling above and below the zero delta latitude line gives the probability of seeing an event above those thresholds integrated over a delta latitude poleward (positive delta latitude) or equatorward (negative delta latitude) starting at that CG latitude. The bar graph at the bottom gives the number of passes in which an event was seen in each of the 20 CGL zones.

For this example, one sees that the maximum probability of seeing an event within a single CGL zone occurs between 66 and 68° CGL (approximately 1.4 percent). Integrating poleward of that latitude over a delta latitude of 8° increases that probability by approximately a factor of 3. Similarly, integrating equatorward of that latitude over a delta of 6° approximately doubles the probability. The minimum spatial integration required to obtain the highest probability of approximately 5.6 percent is approximately 30° CGL starting at 58° CGL and integrating poleward or 25° starting at 75° and integrating equatorward.

We next consider how the maximum and integral probabilities vary as a function of the variation of thresholds and spatial and activity separations. We first examine the variation with changes in the integral energy flux threshold. For this case, we take an average energy threshold of 7 keV for the 2100-2400 MLT sector and for the Kp range from 2- to 3+. The results are summarized in Table 3 and are shown as gray scale plots in Figures 4 through 9. In the table, the left to the right columns are the energy flux thresholds, the maximum probability seen in a single 2° latitude zone, the corrected geomagnetic latitude of the maximum, whether a 6° latitude integration from the maximum probability gives the largest value for integrating poleward (N) or equatorward (S), the probability this integration gives, and the largest integral probability possible.

For this case, at lower integral energy flux thresholds, the maximum probability is found at a latitude of 65° CGL and moves to 67° for the 50 and 160 kR thresholds. This probability decreases with increasing integral energy flux thresholds, dropping from 9 percent at the lowest threshold to 0.3 percent at the highest. Starting at the maximum probability point and integrating northward over a delta latitude of 6°, these probabilities can be significantly

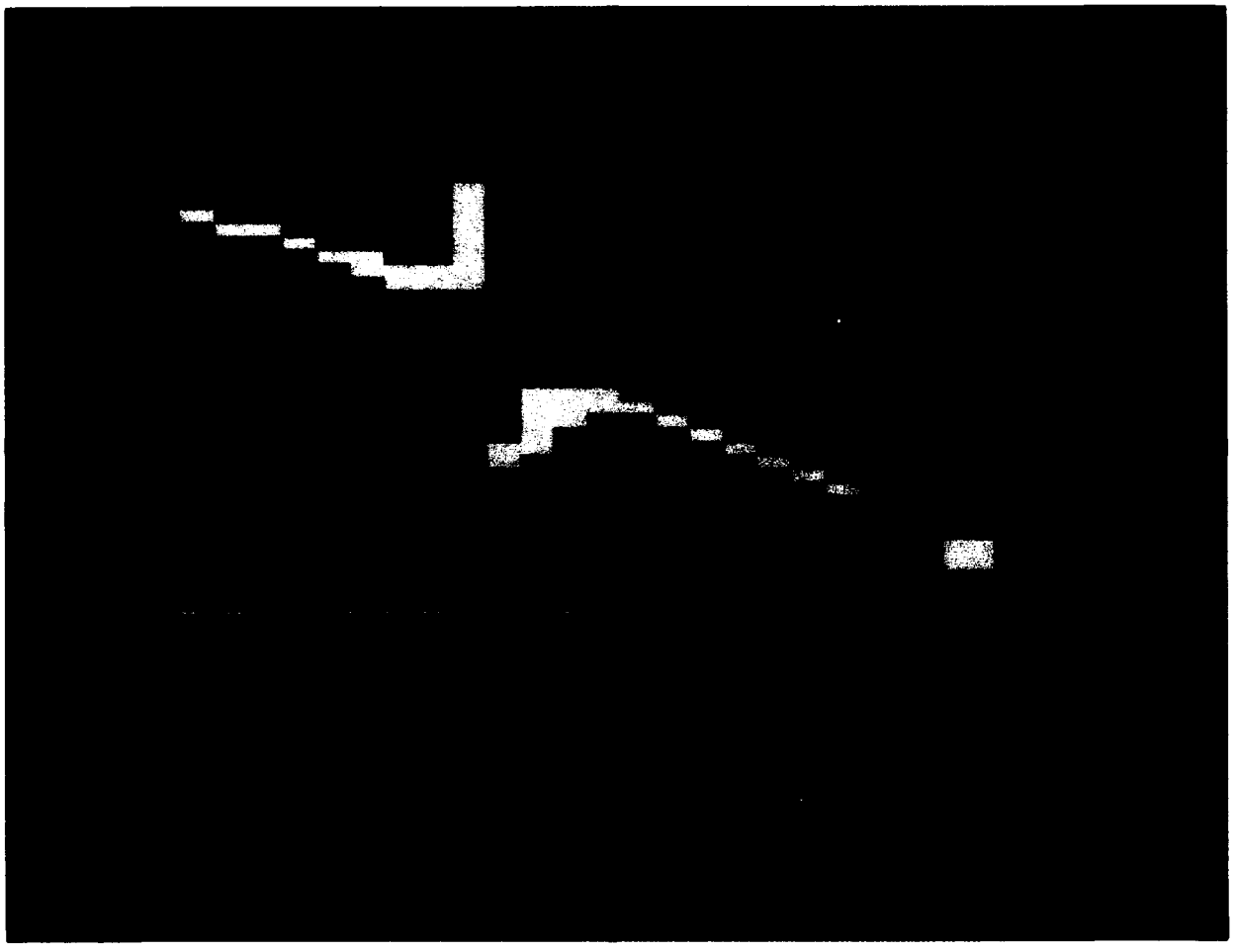

Figure 3. A Typical Plot of the Integral Probability of Auroral Electron Flux Events. The parameter ranges are provided in the legend.

Table 3. Maximum Probability as a Function of JE_{tot}

JE_{tot} Threshold (ergs/cm^2 sec-ster)	Maximum Zonal Probability	CGL	Poleward/ Equatorward Direction	± 6° Δ CGL Probability	Maximum Integral Probability
0.5	9	65	N	12.6	16.2
1.6	9	65	N	12.6	16.2
5	8	65	N	12.8	14.4
16	2.4	65	N	7.2	9.6
50	1.4	67	N	3.5	6.6
160	0.3	67	N	1.2	2.7

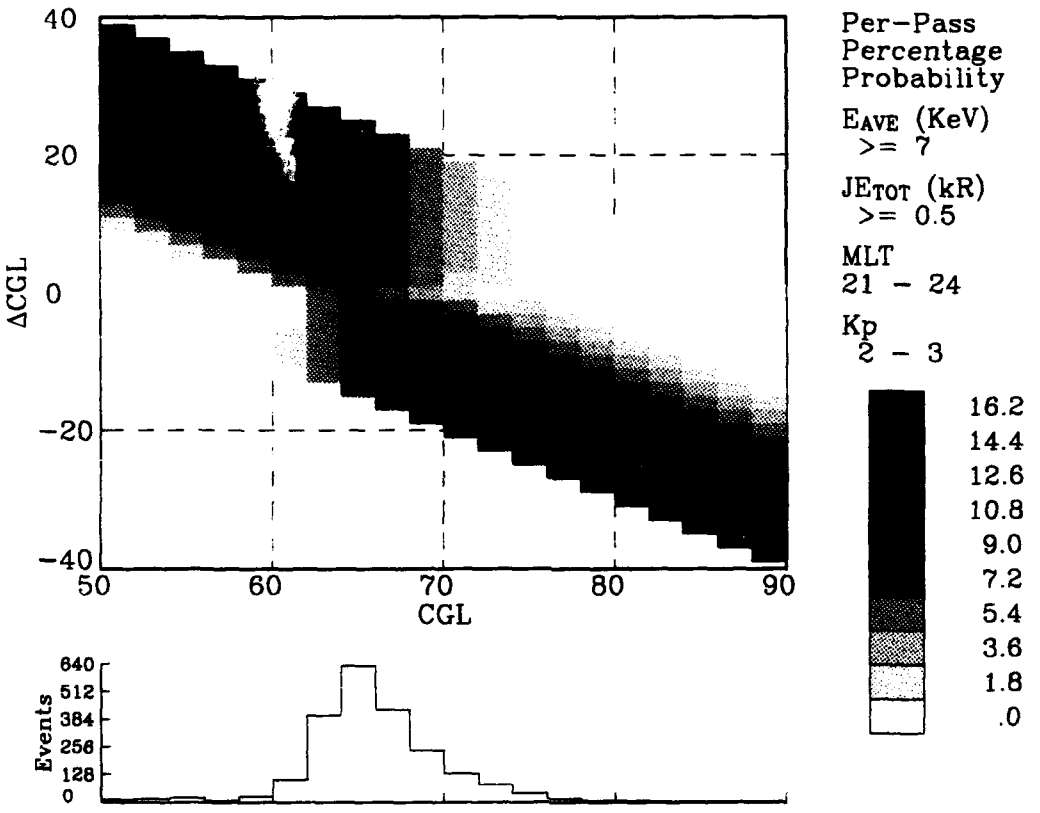

Figure 4. Integral Probability of Auroral electron Flux Events Greater or Equal to 0.5 kR (or 1.0 erg/sec ster). Other parameter ranges are provided in the legend.

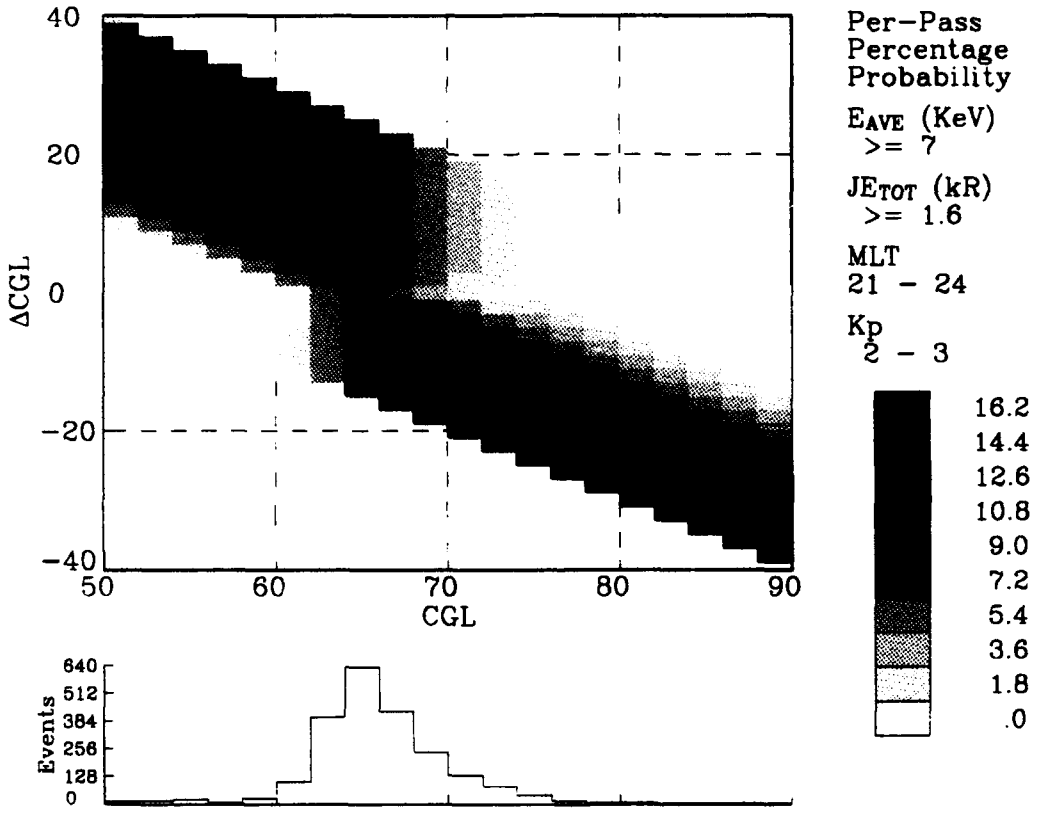

Figure 5. Same as Figure 4 Except that the Energy Flux $JE_{tot} \geq$ 1.6kR (or 3.2erg/sec ster).

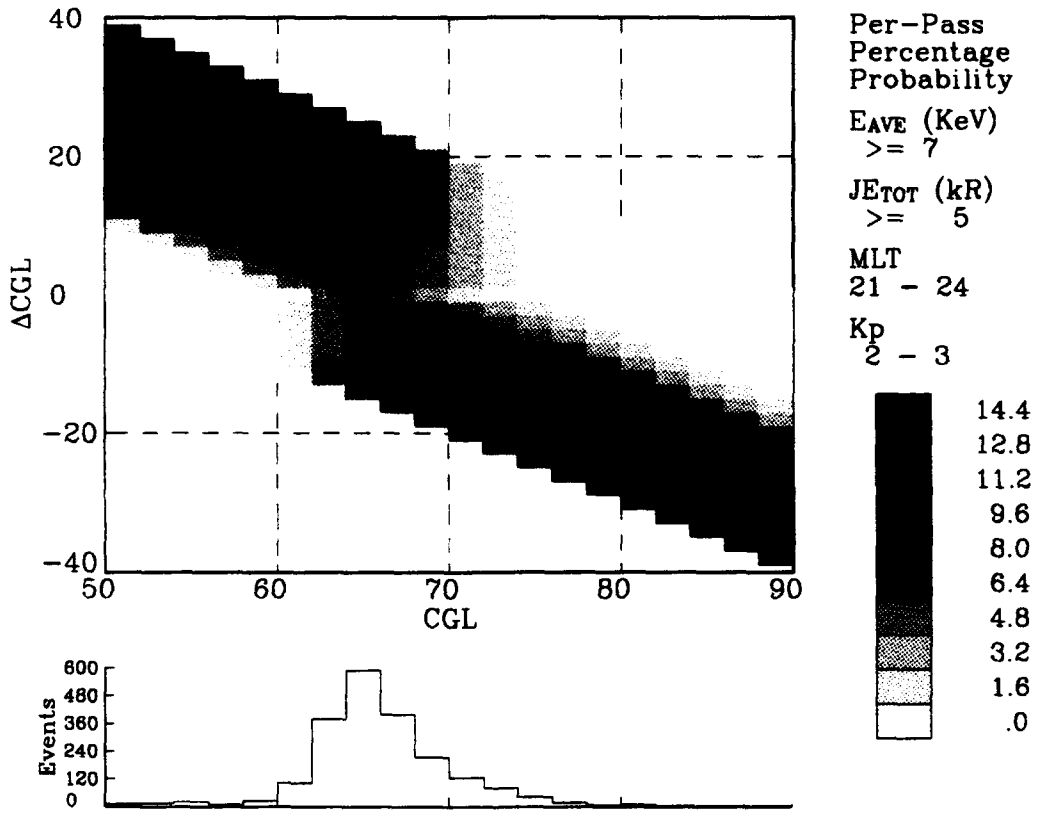

Figure 6. Same as Figure 4 Except that the Energy Flux $JE_{tot} \geq$ 5.0 kR (or 10.0 erg/sec ster).

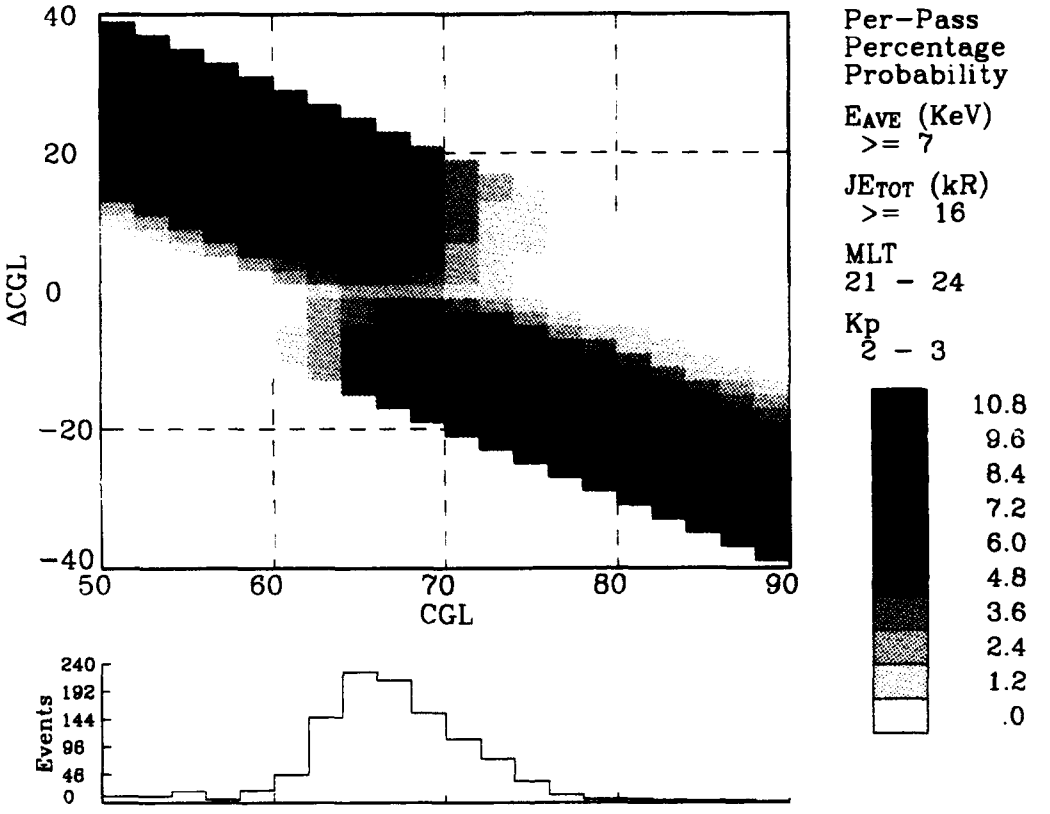

Figure 7. Same as Figure 4 Except that the Energy Flux $JE_{tot} \geq$ 16.0 kR (or 32.0 erg/sec ster).

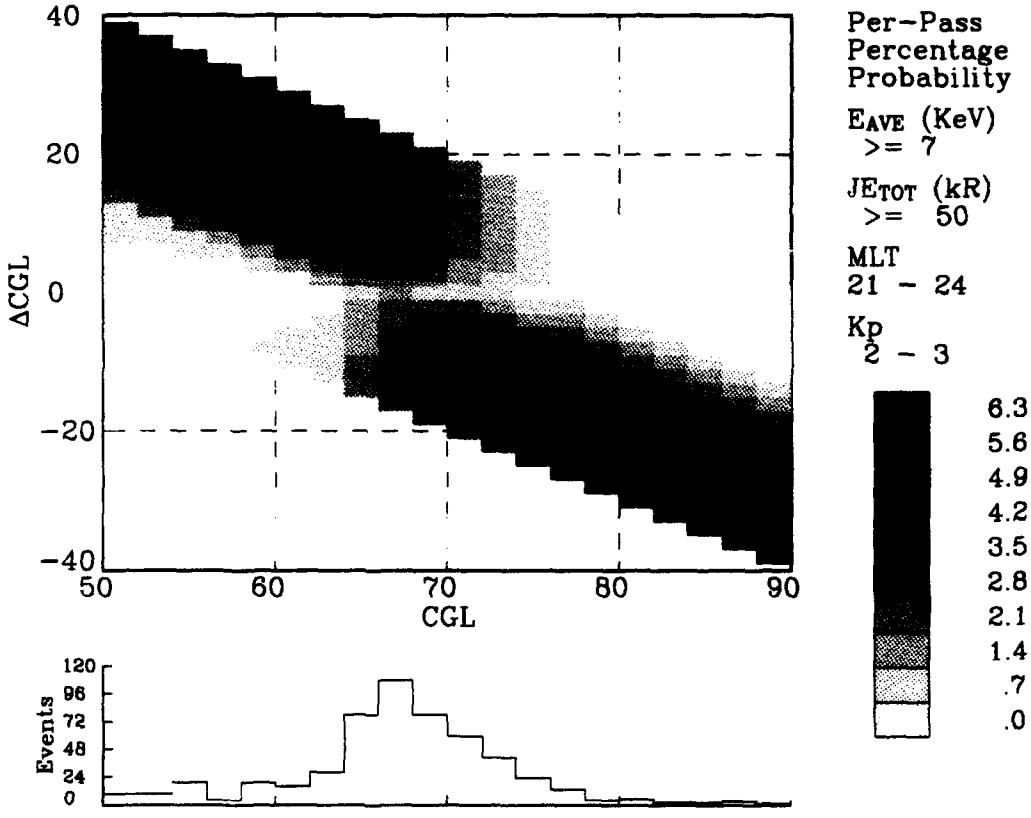

Figure 8. Same as Figure 4 Except that the Energy Flux $JE_{tot} \geq$ 50.0 kR (or 100.0 erg/sec ster).

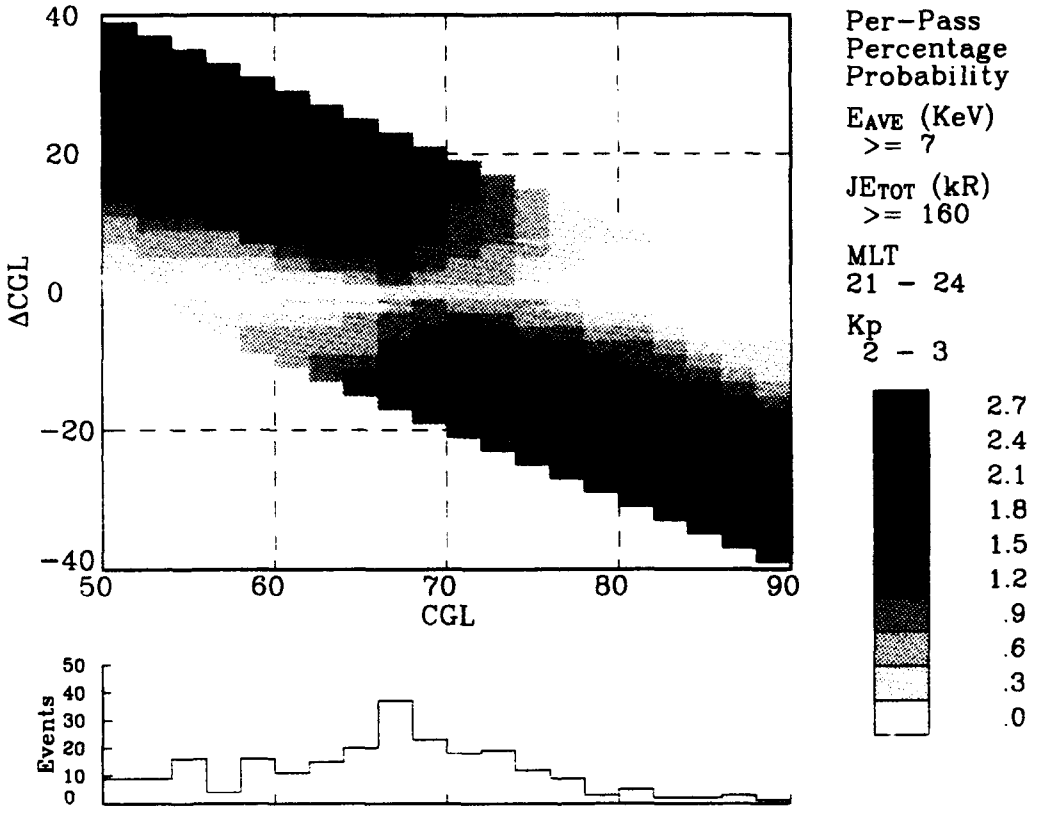

Figure 9. Same as Figure 4 Except that the Energy Flux $JE_{tot} \geq$ 160.0 kR (or 320.0 erg/sec ster).

increased. For the three lowest thresholds the increase is approximately 50 percent. For the higher thresholds the increase can be as much as a factor of 4. The maximum spatially integrated probabilities are even larger, varying from 16.2 percent at the lowest threshold (approximately a factor of 2 increase) to 2.7 percent at the highest threshold (approximately a factor of 9 increase).

We next consider the case where we vary the average energy threshold. For this case we choose an integral energy flux threshold of 5 kR for the Kp range of 2- to 3+ and for the MLT sectors 2100-2400 MLT and 0600-0900 MLT. The results are summarized in Table 4. For both local time sectors the maximum probability decreases with increasing average energy, falling from 12 to 0.2 percent for the 0600-0900 MLT sector and from 20 to 0.2 percent for the 2100-2400 MLT sector. For the 0600-0900 MLT sector the location of the maximum moves to a lower latitude with increasing average energy while for the 2100-2400 MLT sector, the maximum is located at 65° CGL for all but the largest average energy. As for the previous case, the probabilities are significantly increased by integrating over latitude. Integrating over 6° from the maximum increases the probability by 50 to 60 percent at the lower three thresholds for both MLT sectors and by more than 100 percent at the highest thresholds.

Table 4. Maximum Probability as a Function of E_{ave}

E_{ave} Threshold	Maximum Zonal Probability	CGL	North/South Direction	± 6° ΔCGL Probability	Maximum Integral Probability
0600-0900 MLT					
1	12	69	N	18	27
3	10	69	S	15	20
7	9	67	N	12.6	16.2
10	4	67	S	7	9
13	1.05	65	N/S	1.75	3.5
17	0.2	65	S	0.6	1.0
2100-2400 MLT					
1	20	65	N	32	36
3	14	65	N	24.5	28
7	8	65	N	12.8	14.4
10	3.2	65	N	4.8	7.2
13	1.05	65	N	2.1	3.5
17	0.2	67	N	0.8	1.6

Lastly, we consider the case where the thresholds and MLT sector are held constant and the Kp range is varied. For this case the integral energy flux threshold is 5 kR, the average energy

threshold is 7 keV and we looked at the 2100-2400 MLT and 0600-0900 MLT sectors. These results are summarized in Table 5. One notes that for these thresholds the maximum probabilities for both local times occur for Kp in the range from 2- to 3+. The values of the maximum probability for the two cases are also approximately the same for the MLT sectors. The location of the maximum probability moves equatorward in latitude with increasing activity in both MLT's; from 67 to 63° for the 0600-0900 MLT sector and from 67 to 61° for the 2100-2400 MLT sector. This behavior is consistent with the known expansion of the oval to lower latitudes with increasing activity. The increase in the probability with the integration in latitude is much the same as for the previous cases shown.

Table 5. Maximum Probability as a Function of Kp

Kp range	Maximum Probability	CGL	North/South Direction	± 6° ΔCGL Probability	Maximum Integral Probability
0600-0900 MLT					
$0_0 \rightarrow 1+$	0.7	67	S	1.4	3.15
$2- \rightarrow 3+$	9	67	N	12.6	16.2
$4- \rightarrow 5+$	4.5	65	N	7.2	8.1
$6- \rightarrow 9_0$	0.6	63	N	1	1
2100-2400 MLT					
$0_0 \rightarrow 1+$	7	67	N/S	2.10	3.15
$2- \rightarrow 3+$	8	65	N	12.8	14.4
$4- \rightarrow 5+$	4.5	63	N/S	6.3	8.1
$6- \rightarrow 9_0$	0.75	61	N/S	1.2	1.5

4. CONCLUSION

A statistical study has been completed using the SSJ/4 data from the F9 DMSP satellite. The results of the study provide the capability to determine, for locations about the auroral oval, the probability of observing auroral electron precipitation above specified levels in the integral energy flux and average energy for any line of sight through the oval. This provides a new tool for satellite flight mission planners to determine the pointing of onboard systems to maximize the probability of observing specific levels and types of auroral phenomena. More importantly, the results provide the capability to determine for operational Air Force systems the probability that auroral precipitation at specific level is producing background to surveillance systems operating through the oval or ionospheric perturbations for C^3I operating in and through the auroral oval.

The only deficiencies in the present study arises from the use of only one year of DMSP F9 SSJ/4 data. The use of only the SSJ/4 data from the F9 satellite limits the magnetic local time coverage of the study and the use of only one year limits the statistical accuracy of the results. These problems can be eliminated through the use of data from the SSJ/4 detectors on the F7, F8, F10 and F11 satellites. In combination, these instruments have recorded many years of data and provide nearly complete MLT coverage of the oval. Such an extension of the present study remains an option.

References

1. Hardy, D.A., Gussenhoven, M.S. and Holeman, E. (1985) A statistical model of auroral electron precipitation, *J. Geophys. Res.*, **90**:4229.

2. McNeil, W.J., Hardy, D.A., and O'Neil, R.R. (1984) Private communication, 4 September.

3. McNeil, W.J., and Hardy, D.A. (1985) Private communication, 17 October.

4. Hardy, D.A., Gussenhoven, M.S., Raistrick, R. and McNeil, W.J. (1987) Statistical and functional representations of the pattern of auroral energy flux, number flux, and conductivity, *J. Geophys. Res.*, **92**:12275.

5. Hardy, D.A., Gussenhoven, M.S. and Brautigam, D. (1989) A statistical model of auroral ion precipitation, *J. Geophys. Res.*, **94**:370.

6. Hardy, D.A., McNeil, W.J., Gussenhoven, M.S. and Brautigam, D. (1991) A statistical model of auroral ion precipitation 2. Functional representation of the average patterns, *J. Geophys. Res.*, **96**:5539

7. Brautigam, D.H., Gussenhoven, M.S., and Hardy, D.A. (1991) A statistical study on the effects of IMF B_Z and solar wind speed on auroral ion and electron precipitation, *J. Geophys. Res.*, **96**:5525.

8 Jursa, A.S., Scientific Editor (1985) *Handbook of Geophysics and the Space Environment*, Chapter 12, AFGL-TR-85-0315, AD A167000

Appendix

Description of the PC Software EPDF9

The software that generates the integral probability plots is interactive and is menu-driven using the binned data base containing the total number of auroral event occurrences. This software was tested on a IBM PC. The graphic development was based on a commercial graphics package (GraphiC by Scientific Endeavors Inc.). Installing the software in other PC machines is a simple procedure. The EPDF9 software uses a menu with several options given in Table A1. The first four options set the auroral parameter ranges. These parameters are the energy flux threshold, the average energy threshold, the magnetic local time sector, and the Kp range. Option 5 initiates the plot once the parameters have been selected. Option 6 is to save the plot (*.TKF) and listing (*.LST) files. Option 7 makes it possible to display the results on the screen or generate a laser copy. Option 8 exits the program. Option 9 indicates that the user has finished selecting the parameters.

Table A2 lists the possible inputs for each option. The value to be given as the input is the number in parentheses for each of the first four options. The user is asked to change the parameter values of the options that were selected in the previous menu. The program interprets all options in the order selected or until a plot is requested. The plots are then generated on request. The program again displays the menu in Table A1 if no plot is requested or after each plot is completed. This procedure is repeated until the user selects Option 8, which ends the session.

The results are displayed in terms of integral probability versus latitude zones for a fixed local time sector, average energy and energy flux thresholds. The probabilities are referred to as the per-pass probability since they are derived from measurements collected during individual

individual hemispheric passes. The number of events observed in each latitude zone is also shown in a histogram in the bottom of each plot. This histogram should indicate how reliable the computed probabilities are. The gray scale plots were generated for this document on the HP LaserJet III.

Table A1. EPDF9 Menu

1) JEtot	2) Eave	3) Local Time
4) Kp Range	5) Start Plot	6) Save Files
7) Screen/Printer	8) Quit Session	9) Done with Selection

Table A2. EPDF9 Option Description

Option	Description
1	Energy Flux Thresholds in kR (1) 0.5 (2) 1.6 (3) 5.0 (4) 16.0 (5) 50.0 (6) 160.0
2	Average Energy Thresholds in keV (1) 1.0 (2) 3.0 (3) 7.0 (4) 10.0 (5) 13.0 (6) 17.0
3	local time 3-hour sector (1) 0 - 3 (2) 3 - 6 (3) 6 - 9 (4) 9 - 12 (5) 12 - 15 (6) 15 - 18 (7) 18 - 21 (8) 21 - 24
4	Kp index range (1) 0_0 _ 1+ (2) 2- _ 3+ (3) 4- _ 5+ (4) 6- _ 9_0
5	Generate plot and listing
6	Save plot (.TKF) and listing (.LST) files
7	Screen (0) or Laser Printer (1) Option
8	Terminate Session
9	Quit Menu

We next illustrate a typical sample run. To be able to run EPDF9 on a PC system, the following files must be available in the default directory:

EPDF9.EXE	main executable program
MSXDBA.DAT	binned DMSP data file
MSXPSD.DAT	total number of passes in each spatial grid
*.FNT	graphics font files
*.DRV	graphics screen files
*.PRN	graphics printer files
SAVER.BAT	batch file to save plot and listing files

The following steps illustrate a sample run of the EPDF9 software.

Step 1: Type EPDF9 and a menu is displayed as in Table A1. We choose the following options for this session:

1 3 2 4 5 9

These options will be executed in the order given. The first four options request changes of the energy flux JE_{tot} threshold, the MLT sector, the average energy E_{ave} threshold, and the Kp range, in this order. Option 5 is then requested for generating a screen plot (which is the default at the beginning of each session). Option 9 is terminate the input selections.

Step 2: *Option 1:* To change JE_{tot} threshold, use one of the values in Table A2. We choose bin # 4; *i.e.*, all energy fluxes greater or equal to 16 kR. Note that to keep the current JE_{tot} range, enter any negative integer value can be entered.

Option 3: To change MLT sector, use one of the values in Table A2. We choose bin # 8; *i.e.*, all measurements that were recorded in the 2100 to 2400 MLT sector. Again to keep the current MLT sector, enter any negative integer value.

Option 2: To change the average energy E_{ave} threshold, use one of the values in Table A2. Use the default value (bin # 1) by entering any negative integer. This means that all measurements with E_{ave} greater or equal to 1 keV are considered. Note that option 2 comes after option 3 due to the selection order in step 1.

Option 4: To change the geomagnetic activity Kp range, use one of the ranges in Table A2. In this case, two values must be entered. We choose the lower bound and the upper bound of Kp to be in bin # 2; *i.e.*, all measurements that were recorded when Kp was between 2- and 3+.

Option 5: This option generates a plot. Since option 7 was not selected, a plot on the screen will be generated, which is a default at the beginning of each session.

At this point, the data is read in and the appropriate steps are taken to generate the percent probabilities for the specified electron event.

Step 3: After examination of the plot, pressing the RETURN/ENTER key displays the menu in Table A1 as in Step 1. We may select Option 6 to save the listing and plot files or generate an HP laser copy of this plot. To generate a hardcopy, we enter the 7, 5, 9 choices, in this order.

Step 4: *Option 7:* To obtain a hardcopy of this plot, we choose the printer option by entering 1.

Option 5: Generates the plot and sends the results to the HP laser printer. This plot is shown in Figure A1. The integral probability versus latitude is given on the top panel of Figure A1 for this electron event. The cut-off of each probability range is given by a shaded pattern on the right-hand side of the figure. The horizontal axis shows the corrected geomagnetic latitude (CGL) in degrees. The vertical axis gives the offset in degrees from CGL; in other words, the vertical axis is the delta latitude (ΔCGL). When ΔCGL is not zero, the probability value is the cumulative probability from ΔCGL=0 to this latitude offset. Positive ΔCGL means that we are looking poleward from CGL. Negative ΔCGL means that we are looking equatorward from CGL. The bottom panel shows the number of occurrences of the electron events over all latitude zones.

Step 5: After the plot is generated, pressing the RETURN/ENTER key again displays the menu in Table A1. To terminate the session, we type in 8.

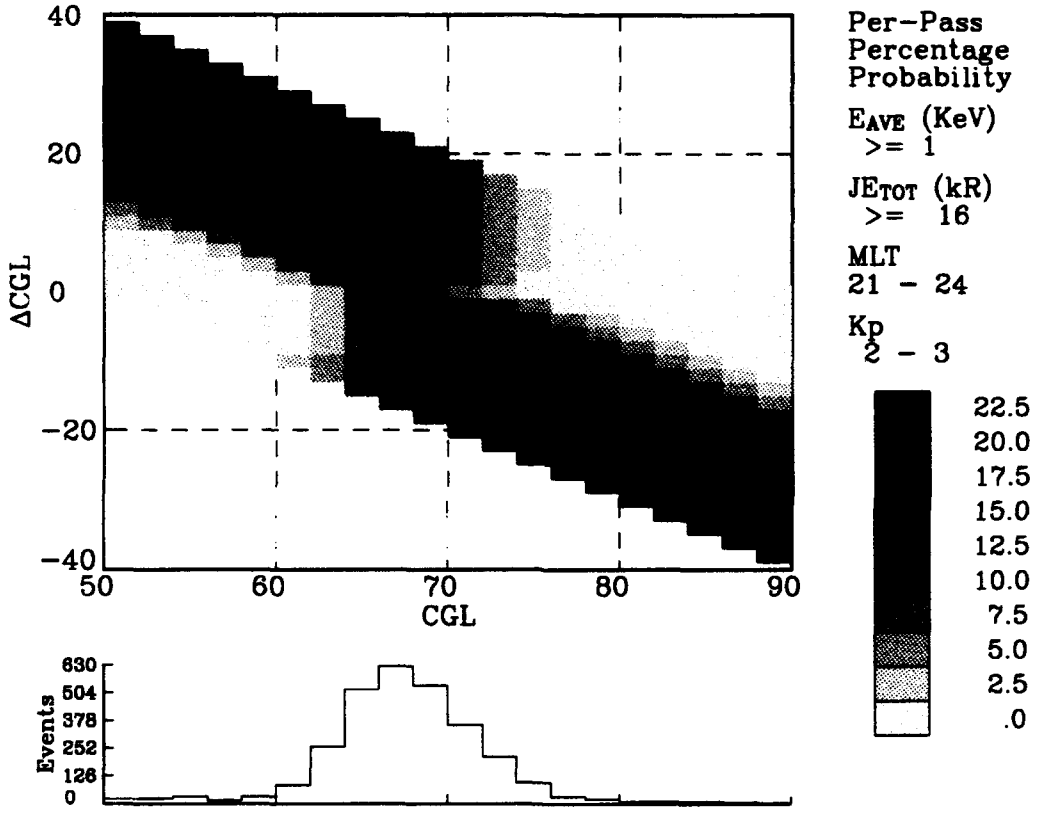

Figure A1. Sample Plot of the Integral Probability of the Auroral Precipitating Electron Events with the Parameter Ranges Provided in the Legend.